OPTIMAL SPINDLE SPEED MACHINING BASED ON ADAPTIVE STABILITY ANALYSIS

Chih-Chun Cheng, Yin-Chun Cheng, Yu-Sheng Chiu, Wen-Nan Cheng and Ping-Chun Tsai

Advanced Institute of Manufacturing with High-tech Innovations and Department of Mechanical Engineering, National Chung Cheng University, No. 168, Sec. 1, University Rd., Ming-Hsiung, Chia-Yi 62102, Taiwan, R.O.C.
email: imeccc@ccu.edu.tw

Cheng-Kuo Sung

National Tsing Hua University, Department of Power Mechanical Engineering , No. 101, Section 2, Kuang-Fu Road, Hsinchu, 30013, Taiwan, R.O.C.

A stable machining technique using adaptive spindle speed is proposed, where the spindle speed is adjusted optimally according to an on-line machining stability analysis. With two accelerometers attached on the spindle, the dynamic characteristics, i.e. the natural frequency and the associated damping corresponding to the spindle-tool system coupled with the cutting impedance, are identified during the machining process using the operational modal analysis (OMA). With this information, the stability lobe diagram (SLD) which determines the optimal spindle speed is obtained and then the spindle speed is on-line adjusted accordingly. This proposed adaptive spindle speed machining technique is integrated with CNC controller and its performance in machining is assessed experimentally.
Keywords: stability lobe diagram, operational modal analysis, natural frequency, accelerometer

1. Introduction

In metal cutting the primary objective aims to have a high material removal rate (MRR) with a satisfactory surface quality. However, the machining instability such as chatter that causes poor work-piece surface roughness and tool wear in the machining process is always an important issue to be addressed. The mechanism of chatter and the technique to avoid it have been studied for many years [1-5]. Practically the operator of a machine tool wants to know two cutting parameters i.e. the depth of cut and the spindle rotational speed before starting a machining process. However, to create the stability lobe diagram (SLD) which provides the crucial information of depth of cut and spindle rotational speed for a stable machining requires the information of cutting force and the frequency response function (FRF) [2]. Nevertheless, the pricy dynamometer is not possible to be installed on ordinary machine tools in market except for the research purpose in lab. On the other hand, the FRF traditionally is obtained through the impact testing of experiment modal analysis (EMA). While the impact testing is conducted, the modal parameters identified is in idle, which are different from those obtained during the machining process. Besides stiffness variation induced by the spindle rotational effect, the difference attributes mainly due to the change in boundary conditions; i.e. the cutting conditions presented at the tool-work-piece interface during the machining [4, 5]. To take the influence of spindle rotational effect and the cutting condition into account, the modal parameter of a spindle-tool system should be estimated during the machining process, which the classic EMA cannot be conducted. To accomplish this task of acquiring the modal parameters of a spindle-tool system during the machining, the operational modal analysis (OMA) which identifies the structural modal parameters only from the output response becomes a good choice.

OMA has been adopted to determine the dynamic properties of a machine tool including tool, spindle, and machine frame which change during operation [6]. However, the classic OMA has an assumption of white noise excitation and it greatly restricts the practical applications as well as its reliability. In recent year, an improved OMA method based on transmissibility measurements which does not make any assumption about the nature of the excitations to the system is introduced [7, 8]. By combining transmissibility measurements under different loading conditions, it is shown that modal parameters can be identified while the excitation contains harmonics.

This paper presents an adaptive spindle speed machining technique, which utilizes the transmissibility based OMA to determine the modal parameters of spindle-tool system coupled with the cutting impedance during the machining. With the information of modal parameters, the SLD is created and then the optimal spindle speed can be determined. It is worth of noting that the detection of modal parameters is continuous during the machining. Subsequently, the spindle speed is adjusted ceaselessly according to the SLD updated continuously during the machining in order to guarantee a possible stable machining.

2. Machining instability from impedance point of view

For a spindle-tool system during a machining process, Figure 1 depicts a schematic model of the interaction between three subsystems represented respectively by their mechanical impedances, i.e. the workpiece Z_w, the spindle-tool system Z_g and their interaction modeled as the cutting impedance Z_c, where the cutting impedance is $Z_c = -jK_c/\omega + C_c$, K_c is the cutting stiffness, C_c is the processing damping, the spindle-tool system $Z_g = j(M_g\omega - K_g/\omega) + C_g$, M_g, K_g and C_g are the equivalent mass, stiffness and damping, respectively. Notice that the processing damping C_c and the stiffness K_c at the interface between the cutting tool and machined surface are assumed to be constant for simplification, although they appears to be nonlinear to certain degree during the machining.

To achieve a higher material removing rate without machining instability, i.e. the chatter, is always an important issue in a machining process. The mathematical model that simulates the regeneration of waviness on the workpiece is represented by a delayed differential equation, i.e. $h(t)=h_0-w_p(t)+\mu w_p(t-T)$, where T is the rotation period of the workpiece, h_0 is the static chip thickness, μ is the overlap factor, $w_p(t)$ and $w_p(t-T)$ are the present and past vibration amplitudes of the workpiece in the radial direction, respectively. With Laplace transform, the transfer function which defines the ratio between the general dynamic chip thickness $h(t)$ and the static chip thickness $h_0(t)$ is given by [9]

$$\frac{h(s)}{h_0(s)} = \frac{1}{1 - G/G_{CP}}, \tag{1}$$

where $G_{CP}(\mu, T) = -1/(1-\mu e^{-j\omega T})$, $G = Z_{gc}/Z_w$, $Z_{gc} = Z_g + Z_c$ is the resulting impedance from the cutting tool and the interface between the tool and the workpiece, i.e. the cutting impedance. Here we cite Cheng's work [9] to numerically illustrate the machining instability. Consider a simply supported beam as a workpiece with Young's modulus E=200 GPa, density ρ=7700 kg/m^3, length L=2 m and diameter d=0.05 m. Assume that the spindle-tool system has a mass twice as large as the workpiece, i.e., M_g=2M and its stiffness and damping are the same as those of the cutting interface, i.e. K_c=K_g=2×10^7 N/m, C_g=C_c=2.6×10^3 N-s/m. A gain-phase plot, i.e. the Merritt curve [1], of the workpiece is shown in Fig. 2[9].

In this figure, varying the excitation frequency to the workpiece, the locus of G_{CP} is denoted by the dotted line whereas G is represented by the solid line. The locus of G appear to be multiple ellipses with each representing a dominating vibration mode of workpiece starting from ω=0 to ω=1000 rad/s in a direction indicated by the arrow. Note that the chatter occurs when the denominator of Eq. (1)

goes to zero, which is represented graphically by the intersections between the loci of G_{CP} and G, i.e. $G = G_{CP}$. It implies that the chatter can be avoided if the loci of G which is controlled by Z_{gc}/Z_w is away from those of G_{CP}. If we can keep G at its minimum, then G has little chance to intersect with G_{CP}. Several methods based on this concept of reducing G have been proposed and implemented practically. One may notice that chatter can be avoided if the spindle keeps running at those speeds where G has its minimal value during the machining process. Nevertheless, $G=Z_{gc}/Z_w$ is a time varying impedance ratio during the machining, so the spindle speed requires to be changed adaptively according to the value of G. It concludes that without adding an additional device to increase the process damping and/or machine stiffness, the chatter can be avoided simply by tuning the spindle rotational speed.

We propose a method to detect the natural frequency of the spindle-tool system coupled with the cutting impedance during the machining by using an on-line operational modal analysis. The natural frequency detection using OMA and then we create the SLD to determine the optimal spindle speed. The spindle rotational speed tuning are performed continuously throughout the machining process.

3. Brief review of operational modal analysis

In a machining process, the excitation to the machine tool is more complex and harmonic components often present in the response. Therefore, applications of conventional OMA encounter difficulties in identifying the modal parameters correctly due to the influence of non-random force contributions. In recent year, an improved OMA method based on transmissibility measurements which does not make any assumption about the nature of the excitations to the system has been introduced [7]. By combining transmissibility measurements under different loading conditions, it is shown that modal parameters can be identified. The transmissibility function $T_{ij}^{k}(s)$ between the output $X_i(s)$ at point i and the reference-output $X_j(s)$ at point j is defined as [7]

$$T_{ij}^{k}(s) = \frac{X_i(s)}{X_j(s)}, \quad i, j = 1, 2, ..., n, \tag{2}$$

where k is the location of an excitation. In general the excitation is unknown and the transmissibility function can be expressed as:

$$T_{ij}(s) = \frac{\sum_{k=1}^{N} H_{ik}(s) F_k(s)}{\sum_{k=1}^{N} H_{jk}(s) F_k(s)}, \tag{3}$$

where N is the total number of excitations applied to the structure, $F_k(s)$ is the excitation at location k and $H_{ik}(s)$ is the transfer function. Assume the structure in resonance, Eq. (3) is reduced to

$$\lim_{s \to \lambda_r} T_{ij}(s) = \frac{\phi_{ir} \sum_{k=1}^{N} L_{kr} F_k(s)}{\phi_{jr} \sum_{k=1}^{N} L_{kr} F_k(s)} = \frac{\phi_{ir}}{\phi_{jr}}, \tag{4}$$

where L_{kr} is the modal participation factor, λ_r and ϕ_{ir} are the system's r^{th} pole and its corresponding eigen-function, respectively. It shows that the displacement transmissibility becomes independent of the excitations, $F_k(s)$. And the relationship revealed by Eq. (4) can be used to estimate the eigen-function or the mode shapes. In order to extract natural frequencies with higher precision, the technique of singular value decomposition (SVD) for transmissibility matrix is utilized [8].

4. Experimental validation of adaptive spindle speed machining

The identification of modal parameters of the spindle-tool system is validated using the transmissibility based OMA in this section. A vertical machining center YCM FV-50T has been used in this study. The cutting tool is NACHI end mill with two flutes and the workpiece is a precipitation-hardened aluminium alloy 6061.

4.1 Experimental validation of spindle-tool system in idle

The modal parameters of spindle-tool system is identified when the spindle is idle. The classical impact testing of EMA as illustrated in Fig. 3(a) and 3(b) is conducted when the spindle-tool system is stationary. The tool tip is excited by the impact hammer and the vibration modes and the frequency response function, i.e. the driving point mobility in this experiment are measured. It shows that the natural frequency at 3423 Hz and 3402 Hz are identified to be the yawing modes with the tool tip moving aside in the X-axis and Y-axis directions, respectively. Similarly, the modal parameters of spindle-tool system are also identified through transmissibility based OMA measurements with two accelerometers (PCB 352C22) attached on the spindle and one on the tool tip. Notably only the signals from accelerometers were acquired by the data acquisition (NI 9234) using a sampling rate of 12800 Hz. The natural frequencies and the corresponding mode shapes are calculated according to transmissibility based OMA as described in the previous section coded using MATLAB.

Figures 4(a) and 4(b) show the singular value spectra from OMA in the x and y directions respectively using the transmissibility measurements and then SVD is used for higher accuracy. Curve fitting with 80 orders was adopted in the singular value spectra as denoted in thick solid line and the frequency corresponding to the peak appears clearly to be the natural frequency. Table 1 compares the modal parameters of spindle-tool system on the tool tip corresponding to the first yawing mode obtained from the EMA and OMA, respectively.

With three accelerometers attached in a straight line on the spindle, the mode shape from OMA is confirmed to be the same yawing mode as that in EMA. Furthermore, the difference in the natural frequency in the X-axis and Y-axis directions are 0.2% and 1.4%, respectively; but the modal damping estimated in the Y-axis direction is 46%. With the natural frequency and damping corresponding to the spindle yawing mode identified either by EMA or OMA, the intersection of SLDs respectively derived from the natural frequency and damping ratio identified in the x and y-directions are illustrated in Fig. 5. Notably the right vertical axis of SLD is plotted in terms of stiffness ratio bk_c/k instead of depth of cut due to no cutting force information in the experiment. The SLD from CutPro is also plotted in the same figure with the depth of cut on the left vertical axis for comparisons. The SLD from the modal parameters identified using OMA is intentionally adjusted to the same horizontal positon as that from CutPro. It shows that the difference among them is small and the spindle rotational speed of 7375 RPM is chosen to be an initial spindle speed in the latter machining process.

4.2 Performance assessment of adaptive spindle speed machining

The experiment setup for the machining experiment using the proposed adaptive spindle speed machining is the same as that shown in Fig. 3(b) except that the accelerometer on the tool tip is removed. The cutting parameters are listed in Table 2. The objective is to identify the modal parameters of the spindle-tool system coupled with cutting impedance using the method of transmissibility based OMA during the machining process. Figure 6 illustrates the SVD spectra calculated from the vibration spectra sensed in the radial directions, i.e. the x and y directions, while the machining is in progress. The natural frequency of 3436 Hz and 3450 Hz identified respectively from Figures 6(a) and 6(b) are utilized to plot the SLD as illustrated in Figure 7(a). It shows that the optimal spindle speed should be close to 7422 RPM instead of the initial spindle speed of 7375 RPM obtained when the spindle is idle. The difference in estimating the optimal speed is attributed to the involvement of cutting impedance while in machining. The on-line spindle speed adjustment is continuous according to the SLD updated continuously by the modal parameters identified by OMA during the machining. Figure 7(b) illustrates the SLD created using the modal parameters identified by OMA at the second time during the machining. It shows that the optimal spindle speed should be changed to 7498 RPM.

To assess the performance of the proposed method in stable machining, the workpiece surface roughness and the spindle vibration are compared in varying spindle speeds. Figure 8(a) shows the workpiece surface after machining using spindle speeds, 6580, 7110, 7375 and 7422 RPM, respectively. The acceleration in RMS measured on the spindle corresponding to varying spindle speeds are compared in Fig. 8(b). It shows that the spindle speed changing from the initial 7375 RPM, to the first adjustment of 7422 RPM and to the second of 7498 RPM, the surface roughness and the spindle vibration in RMS are improved successively, which also confirms the feasibility and effectiveness of the proposed method of OMA based adaptive spindle speed machining.

5. Conclusions

A stable machining technique using adaptive spindle speed according to an on-line stability analysis based on the OMA is presented. With two accelerometers attached on the spindle, the dynamic characteristics, i.e. the natural frequency and the associated damping corresponding to the spindle-tool system coupled with the cutting impedance are identified during the machining process using the operational modal analysis based on transmissibility measurements. With this information, the stability lobe diagram which determines the optimal spindle speed is obtained and then the spindle speed is adjusted adaptively. However, precise determination of the varying FRF is vital to create the reliable SLD. Experimental results show that the surface roughness and the spindle vibration are improved successively.

Acknowledgments

This work was supported by Technology of Taiwan, Republic of China under Contract No. MOST 105-2221-E-194-018.

Table 1: Comparisons of modal parameters obtained by EMA and OMA

Method	Direction	Natural frequency (Hz) and mode shape	Damping ratio (%)
EMA	X	3423	1.075
	Y	3402	1.613
OMA	X	3417 (0.2%) [0.001 0.006 1]	1.168 (8.6%)
	Y	3449 (1.4%) [0.003 0.009 1]	0.879 (46%)

Table 2: Machining information in machining experiments

Workpiece	flute	Feed rate (mm/flute)	Depth of cut (mm)	Width of cut (mm)
Al 6061	2	0.12	8	0.3

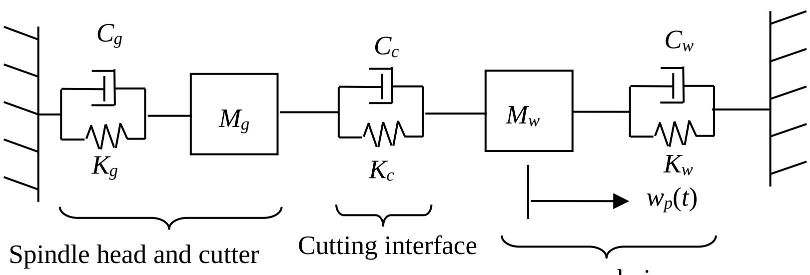

Figure 1: Dynamic couplings between workpiece and spindle-tool system

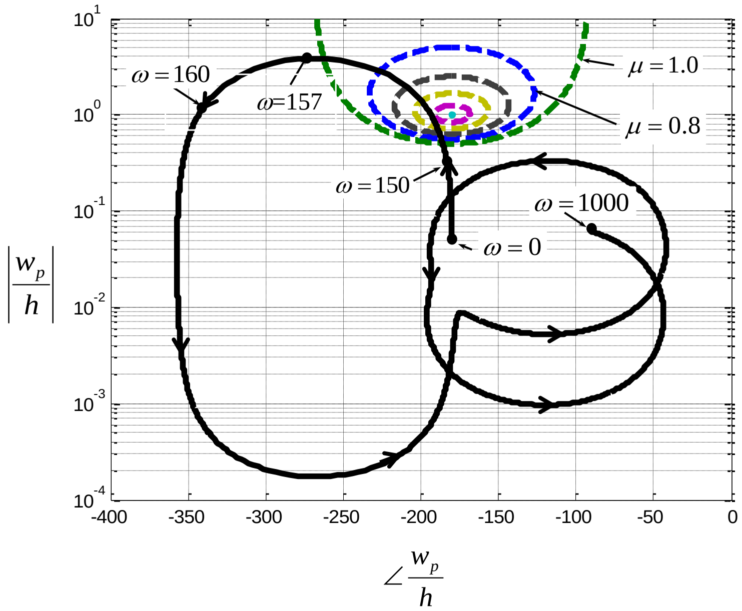

Figure 2: Gain-phase plot of workpiece [9]

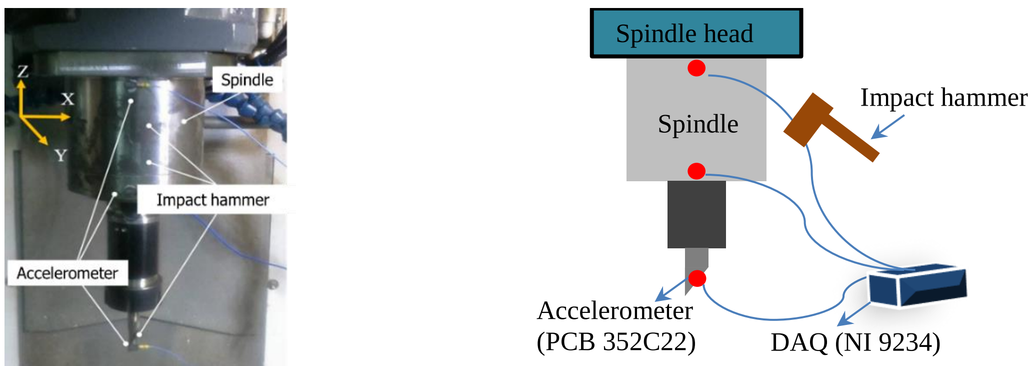

(a) (b)

Figure 3: The modal parameter of spindle-tool system was identified using EMA and OMA; (a) impact testing setup; (b) schematic representation of EMA and OMA

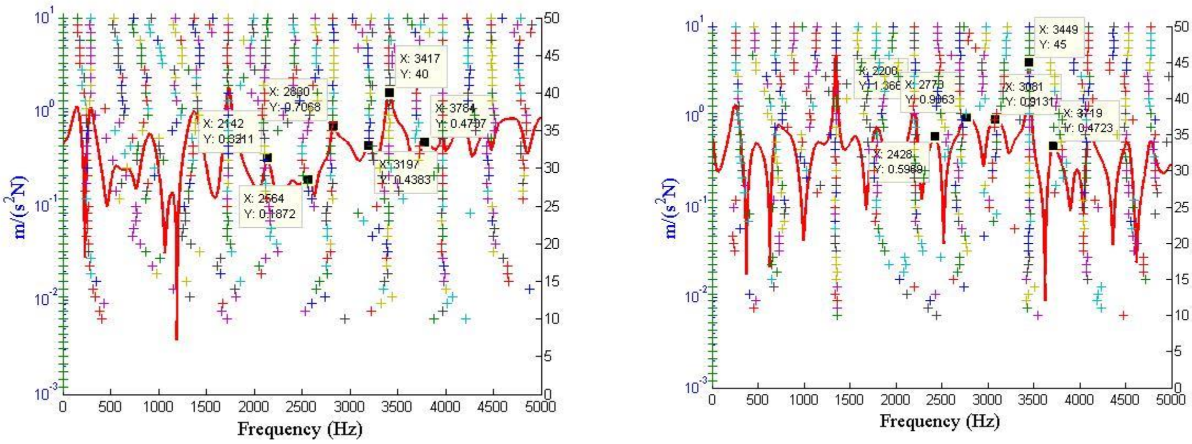

(a) (b)

Figure 4: (a) SVD spectra in x-direction from OMA; (c) SVD spectra in y-direction from OMA

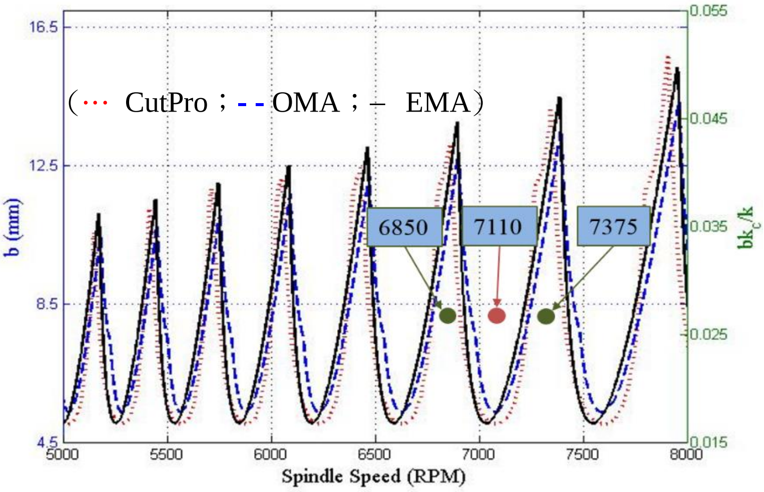

Figure 5: Stability lobe diagram based on the modal parameters identified while the spindle is idle

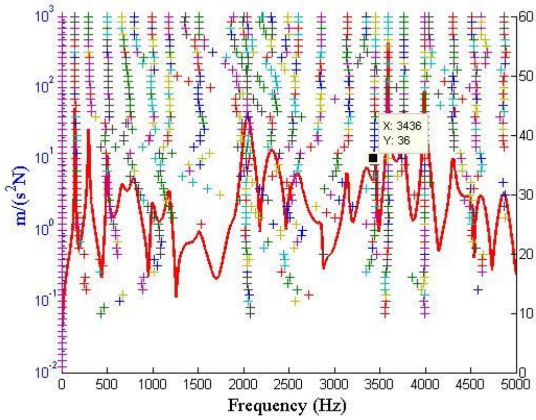

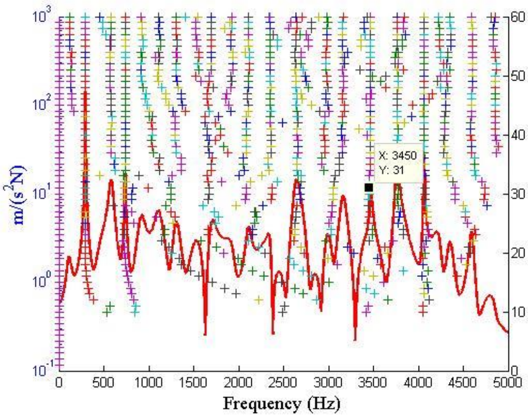

(a) (b)

Figure 6: The first SVD spectra in the (a) x and (b) y directions during the machining

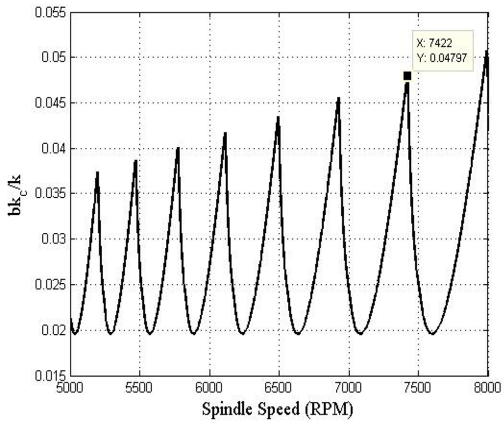

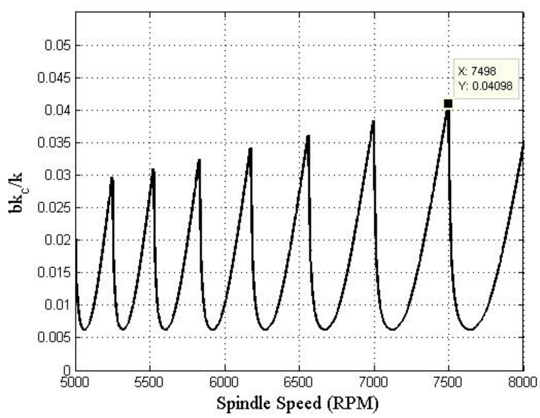

(a) (b)

Figure 7: SLD created using the modal parameters identified by OMA during the machining; (a) first time and (b) the second time

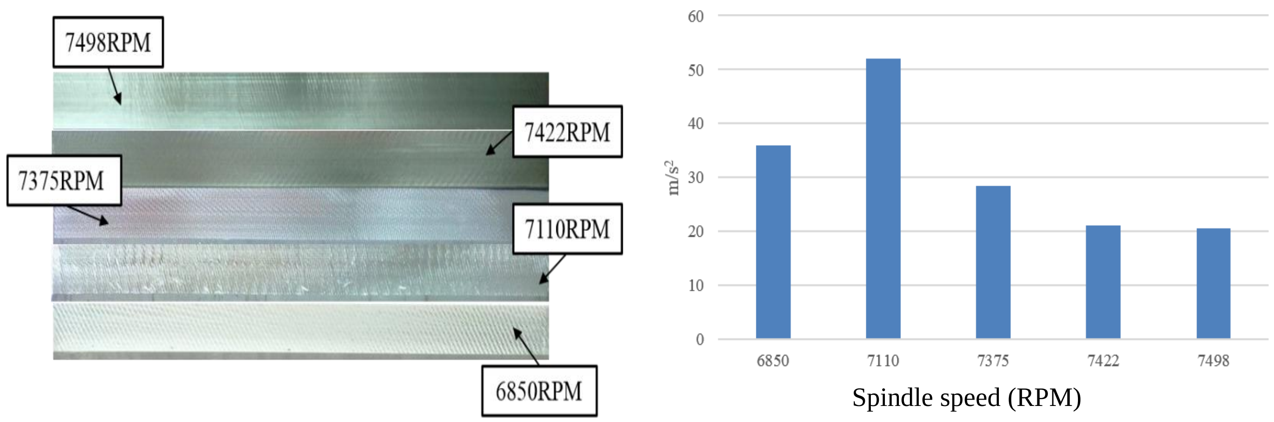

(a) (b)

Figure 8: (a) Workpiece surface at varying spindle speeds and (b) spindle acceleration in RMS versus spindle speed

REFERENCES

1 Merritt, H. E. Theory of self-excited machine tool chatter, *Journal of Engineering for Industry-Transactions of the ASME*, **87**, 447–454, (1965).

2 Altintas, Y. and Budak, E. Analytical prediction of stability lobes in milling, *CIRP Annals*, **44**(1), 357–362, (1995).

3 Jensen, S. A. and Shin, Y. C. Stability analysis in face milling operations. Part1: experimental validation and influencing factors, *Journal of Manufacturing Science and Engineering-Transactions of the ASME*, **121**(4), 600–605, (1999).

4 Gagnola ,V., Bouzgarroua B. C., Raya, P. and Barra, B. Model-based chatter stability prediction for high-speed spindles, *International Journal of Machine Tools and Manufacture*, **47**, 1176–1186, (2007).

5 Jensen, S. A. and Shin, Y. C. Stability analysis in face milling operations. Part 2: experimental validation and influencing factors, *Journal of Manufacturing Science and Engineering-Transactions of the ASME* **121**(4), 606–615, (1999).

6 Zaghbani, I. and Songmene, V. Estimation of machine-tool dynamic parameters during machining operation through operational modal analysis, *International Journal of Machine Tools & Manufacture*, **49**, 947–957, (2009).

7 Devriendt, C. Sitter, G. D., Vanlanduit, S. and Guillaume, P. Operational modal analysis in the presence of harmonic excitations by the use of transmissibility measurements, *Mechanical Systems and Signal Processing*, **23**, 621-635, (2009).

8 Araújo, I. G. and Laier, J. E. Operational modal analysis using SVD of power spectral density transmissibility matrices, *Mechanical Systems and Signal Processing*, **46**, 129-145, (2014).

9 Cheng, C. C., Kuo, C. P., Wang, F. C. and Cheng, W. N. Moving Follower Rest Design Using Vibration Absorbers for Ball Screw Grinding, *Journal of Sound and Vibration*, **326**, 123–136, (2009).